UNITED STATES DEPARTMENT OF THE INTERIOR

GEOLOGICAL SURVEY

Progress report on clay-mineral assemblages in the Gibson Dome No. 1 drill core, Paradox Basin, Utah

By
Marc W. Bodine, Jr. and Bruce F. Rueger[1]

Open-File Report 84-165
1984

This report is preliminary and has not been reviewed for conformity with U.S. Geological Survey editorial standards and stratigraphic nomenclature.

[1]U.S. Geological Survey
Denver, Colorado 80225

TABLE OF CONTENTS

Progress report on clay-mineral assemblages in the Gibson Dome No. 1 drill core Paradox Basin, Utah

By

Marc W. Bodine, Jr. and Bruce F. Rueger

U.S. Geological Survey
P.O. Box 25046, Denver Federal Center, Denver, Colorado 80225

ABSTRACT

Clay mineral analyses of 37 sized separates from 1819 m of cored Mississippian through Permian strata from the Gibson Dome No. 1 drill hole, San Juan County, Utah, yield kaolinite, illite, mixed-layer illite-dioctahedral smectite, chlorite, mixed-layer chlorite-trioctahedral smectite (rare), corrensite, discrete trioctahedral smectite (rare), and talc. Kaolinite is restricted to the paleosol of the Molas Formation and continental beds of the Cutler Formation; discrete illite is restricted to the Lower and Paradox Members of the Hermosa Formation whereas mixed-layer illite-smectite is common-to-abundant in remaining units. Chlorite occurs in marine units and is particularly abundant in the hypersaline Paradox Member of the Hermosa Formation. Talc and abundant corrensite or less regularly interstratified chlorite-trioctahedral smectite are restricted to the Paradox salt lithologies. Variation from terrestrial through normal marine to marine hypersaline depositional environments correlates with changing clay-assemblage chemistries: high alumina through increasing potash and magnesia proportions to dominance of magnesia and substantially reduced alumina, respectively.

INTRODUCTION

A mineralogic and geochemical investigation of clay mineral assemblages through the cored interval in the Gibson Dome No. 1 drill hole is currently in progress. This report contains the results obtained to date as well as some tentative interpretations; the latter are subject to modification or rejection as additional data are obtained.

Gibson Dome No. 1 was drilled and cored for the Department of Energy by Woodward-Clyde Consultants in 1981 to examine the suitability of salt deposits in the Paradox Member of the Hermosa Formation for underground disposal of nuclear waste (Woodward-Clyde Consultants, 1982). The drill hole is located in sec. 21, T. 30 S., R. 21. E, San Juan County, Utah, on the southeast plunging nose of Gibson Dome, a small salt anticline in the Paradox basin. The hole was drilled to a depth of 1946.4 m (6,384.3 ft) and was continuously cored below a depth of 127 m (417 ft) to yield a cored section of 1819 m (5,967 ft); elevation of the Kelly bushing was 1508.5 m (4,949.2 ft) above mean sea level.

STRATIGRAPHY

A stratigraphic log of the Gibson Dome No. 1 drill hole is given on figure 1. Surface rocks at the drill site belong to the Cutler Formation (Permian) and the hole penetrated about 10 m into the Ouray Limestone

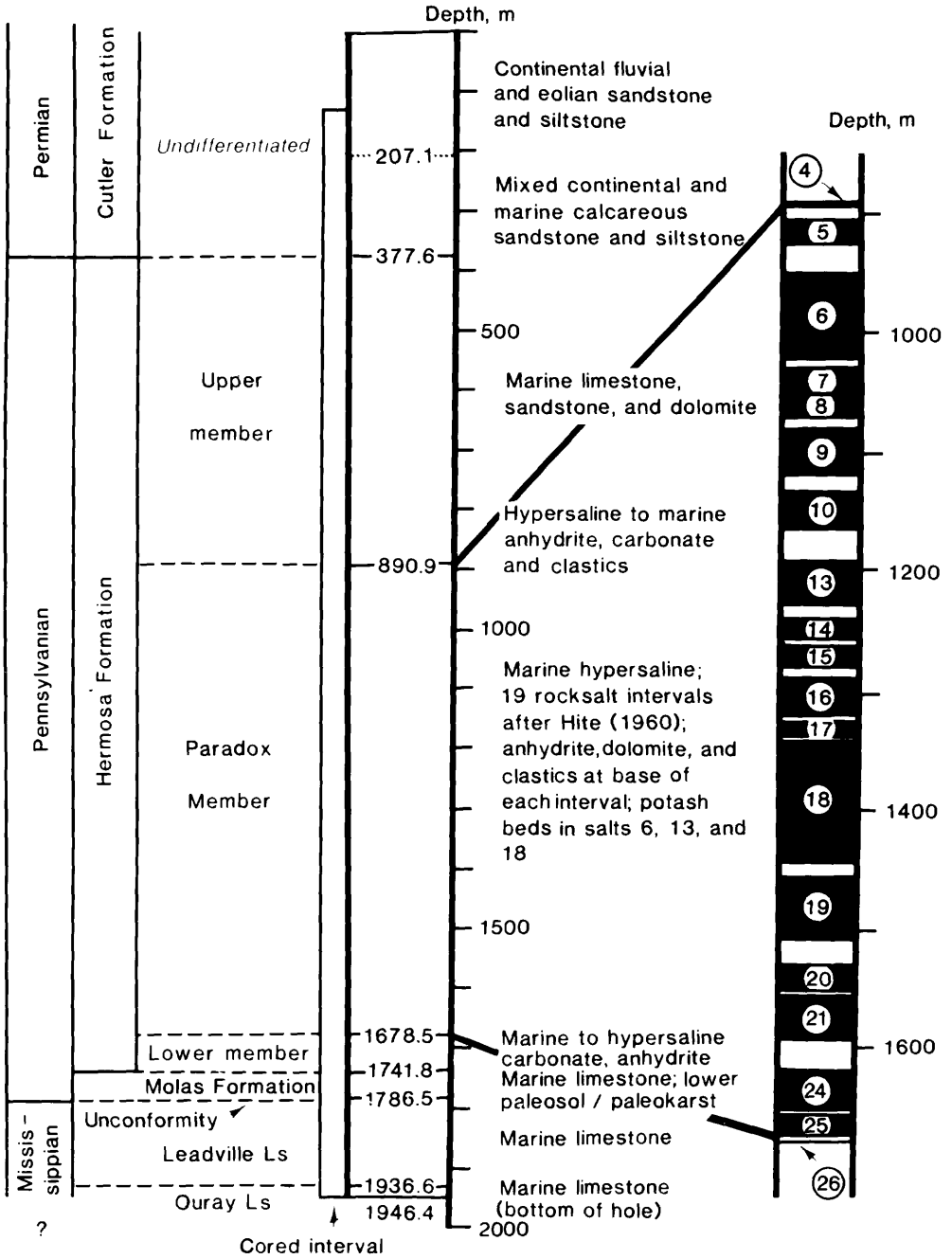

Figure 1.--Stratigraphic column in the Gibson Dome No. 1 drill hole, San Juan County, Utah, (sec. 21, T. 30 S., R. 21 E.) with expanded section of the Paradox Member with Hite's (1960) numbering of the rock salt intervals. [Modified from Woodward-Clyde Consultants, 1982.]

(Devonian-Mississippian). A detailed lithologic log of the hole and an accompanying stratigraphic description are given in Volume II (Gibson Dome) of the geologic characterization report prepared by Woodward-Clyde Consultants (1982); our stratigraphic summary below is abstracted chiefly from their report. Although not incorporating Woodward-Clyde Consultants (1982) nomenclature within the Cutler and Hermosa Formations, we otherwise have observed most of their stratigraphic boundaries and nomenclature.

The Devonian Ouray and Mississippian Leadville Limestones were deposited in an epeiric marine environment. The Ouray Limestone is finely crystalline and contains thin bands and stringers of bluish- to greenish-gray, sporadically pyritiferous shale. The Gibson Dome No. 1 drill hole penetrated 9.8 m (32 ft) into the formation, but did not reach its lower contact. The Leadville Limestone, 149.6 m (491 ft) thick, consists of an upper limestone unit, generally light gray in color and with minor chert; and a lower dolomite unit which contains distinct beds of dolomite, admixtures of dolomite and limestones, and two thin anhydrite beds at depths of 1861 and 1885 m (6,105 and 6,185 ft).

The Molas Formation unconformably overlies the Leadville Limestone and represents initial Pennsylvanian deposition. The lower third of the Molas Formation is a paleosol/paleokarst consisting of clasts of Leadville limestone in a matrix of red mudstone. The overlying Molas lithologies include bedded limestones, shales, and calcareous siltstones; these were deposited in the transgressive Pennsylvanian sea that flooded the previously developed paleosol. The Molas Formation is 45 m (147 ft) thick with the lower 17 m (56 ft) consisting of the paleosol.

The Pennsylvanian Hermosa Formation (Hermosa Group of Wengerd, 1958) overlies the Molas Formation and consists of a lower member (Pinkerton Trail Formation of Wengerd, 1958), the Paradox Member (Paradox Formation of Wengerd, 1958) , and the upper member (Honaker Trail Formation of Wengerd, 1958). Throughout this report we have retained the earlier (Hite, 1960) stratigraphic nomenclature because of unresolved difficulties (see Hite and Buckner, 1980) caused by usage of the Wengerd nomenclature. The lower member is transitional from the upper Molas open-marine environment to the highly restricted hypersaline environment of the Paradox Member. Lower member lithologies include interbedded limestones, dolomites, anhydrites, calcareous siltstones, and shales; the member is 63 m (208 ft) thick. Carbonate lithologies dominate the lower third of the sequence whereas anhydrites and calcareous siltstones dominate the upper two-thirds and reflect the upward increase in salinity of the depositional environment. The contact between the lower member and the overlying Paradox Member is similarly gradational and is placed at the base of the lowest depositional cycle containing a rock-salt interval.

The Paradox Member is 787.6 m (2,584 ft) thick and consists dominantly of halite rock with minor potash salts and substantially smaller amounts of anhydrite, dolomite, silty dolomite, limestone, siltstone, and shale. Deposition of the Paradox Member is distinctly cyclic. Hite (1960) identified 29 cycles in the Paradox Member with each ideally consisting of clastics, carbonates, and anhydrite, that are overlain by a rock-salt interval with or without potash-bearing beds; Hite numbered these cycles, or salt intervals, from 1 (youngest) through 29 (oldest). In the Gibson Dome No. 1 core, all but

10 of the cycles (nos. 1-3, 11, 12, 22, 23, and 27-29) are halite bearing and delineated on figure 1. Thicknesses of the halite intervals range from 2 m (7 ft) in cycle 26 to 105 m (346 ft) in cycle 18; the rock-salt interval in cycle 6, the potential repository horizon, is 73 m (241 ft) thick. In this report, the upper boundary of the Paradox Member was placed at the top of the uppermost halite bed (cycle 4) as suggested by Hite (1983).

Above that boundary (fig. 1), the lower strata of the overlying upper member represent the transition from hypersaline conditions to a normal marine environment. The overlying rocks, almost exclusively light gray to dark gray in color, consist chiefly of fossiliferous limestones with highly variable amounts of clastics and chert; some beds of sandstone, dolomite, siltstone, and claystone also occur. This sequence is dominantly shallow-water marine and transitional with overlying Permian rocks. The thickness of the upper member in the Gibson Dome No. 1 core is 513 m (1,683 ft). In this report, the contact with the overlying Permian was placed at the top of the uppermost fossiliferous marine limestone.

The Permian rocks that overlie the upper member and continue to the surface constitute the upper 378 m (1,239 ft) of the drill hole of which the lower 251 m (823 ft) were cored. In this report, these strata are assigned to the Cutler Formation. In the Gibson Dome area, Woodward-Clyde Consultants (1982) have subdivided this interval into the Elephant Canyon Formation, the Cedar Mesa Sandstone, and an upper sequence of intertonguing Cedar Mesa Sandstone and Cutler Formation lithologies. Although lithologies in this interval suggest affinities to some of these units, several uncertainties exist that make these formational assignments questionable. We prefer to consider the entire sequence above the upper member of the Hermosa Formation as undifferentiated Cutler Formation.

The lower 170 m (560 ft) of the Cutler Formation consist of variegated, generally thin bedded, calcareous siltstones, sandstones, and shales with occasional limestones. The sandstones are often crossbedded, with mica flakes concentrated along bedding planes. The strata commonly contain abundant detrital feldspar, mica, and lithic grains, and are characteristic of immature detritus deposited in a nearshore marine and tidal environment. The upper 207 m (679 ft) consists of calcareous, pale-red to grayish-red sandstones and silty sandstones that are intercalated with red to purplish-red arkosic sandstones; the former were deposited in eolian and tidal environments, and the latter in fluviatile channel environments.

SAMPLING PROCEDURE

Characterization of clay-mineral assemblages in the Gibson Dome No. 1 drill core used a sampling plan with three principal objectives:

1. Sampling the major clay-bearing lithologies in each stratigraphic unit throughout the core.
2. Detailed sampling of the Paradox Member, and in particular, salt 6 (the suggested repository host).
3. Detailed sampling of those stratigraphic that intervals represent changing depositional environments, such as the transition from normal marine to hypersaline conditions reflected in the lower member of the

Hermosa Formation, the transition from hypersaline to normal marine conditions reflected in the lowermost upper member, and the oscillating marine, mixed, and continental environments reflected in the Cutler Formation lithologies.

In this report, we include preliminary results from 37 sampling locations (table 1); and except for the Ouray and Leadville Limestones each formation penetrated by the Gibson Dome No. 1 core hole is represented. Our current laboratory activities, to be reported subsequently, focus on samples from the Ouray and Leadville Limestones, the upper Paradox Member and lower part of the upper member, and upper beds of the Cutler Formation.

CLAY-FRACTION SEPARATION AND ANALYSIS

A 25-250 g split of each sample was crushed and ground to <200 mesh; the amount was based on a visual estimate of clay content. About half of the crushed sample was retained. The other half was thoroughly leached in water to dissolve water soluble salts, then decanted and leached in a boiling 0.2 molal tetrasodium ethylenediaminetetraacetate acid (Na_4-EDTA) solution to dissolve carbonate and Ca-sulfate minerals after Bodine and Fernalld's (1973) procedure. This was followed by three or more cycles of successive centrifugation to sediment all particulates, decanting and discarding the supernatent, and resuspending the residue in distilled water; this produced a suspension of particulates in essentially pure water.

Size fractions of >1 and <1 μm effective spherical diameter (esd) of particulates in suspension were prepared by disaggregation of the sediment with an ultrasonic probe, timed centrifugation, decanting the fine-particle-bearing supernatent from the coarse-particle sedimented residue, and resuspending the residue. We found that the <1 μm effective spherical diameter split was, in most samples, essentially free of quartz, feldspar, and other nonclay minerals, whereas the more conventional <2 μm fraction commonly contained appreciable quantities of the nonclay particulates. One sedimented diffraction mount of the >1 μm fraction was prepared for determining bulk mineralogy of the insoluble fraction.

Oriented sample mounts for diffraction analysis were prepared by vacuum filtering aliquots of sized suspensions through millipore filters to produce thin films of oriented clay flakes on the filters; each film was then transferred onto a glass slide following Pollastro's (1982) technique. This procedure not only yielded more thorough crystallographic orientation of the clay flakes on the mount than the more conventional technique of air-drying drops of the suspension on a glass slide, but also precluded any size bias generated during conventional air-drying in which coarser particles tend to concentrate at the base of the clay film with finer particles concentrated at the top.

Three diffraction mounts of the <1 μm fraction for each sample were prepared: an air-dried mount; a mount saturated with ethylene glycol vapor for 1 hour at 60°C; and a mount heated at 350°C for 1 hour, then, after diffraction, reheated at 550°C for 1 hour. Each mount was scanned with the X-ray diffractometer, and the traces interpreted using standard criteria reported in Brindley and Brown (1980), Carroll (1970), and Grim (1968).

Table 1.--*Mineralogy of clay-mineral assemblages from Gibson Dome No. 1 drill core, San Juan County, Utah*

Formation†	Depth m	Sample number	Host lithology	Clay-mineral assemblage								
				kao	ill	ils	i-s	chl	c-s	cor	sap	tal
Cutler Fm. upper	139.6	GD1-24	Red silty sandstone	XX		XXX						
Cutler Fm., upper	204.8	GD1-28	Red calcareous silty sandstone	XX		XXX		o				
Cutler Fm., lower	213.5	GD1-29	Red calcareous silty sandstone	XX		XXX		o				
Cutler Fm., lower	233.5	GD1-25	Red calcareous sandy siltstone	X		XXX		X				
Cutler Fm., lower	347.5	GD1-26	Red shale	X		XXX		XX				
Cutler Fm., lower	371.9	GD1-30	Red and green calcareous siltstone	X		XXX		XX				
Cutler Fm., lower	374.1	GD1-27	Red shale	o		XXX		XX				
Upper member†	384.4	GD1-33	Brownish-red sandstone			X				XXX		
Upper member†	421.6	GD1-34	Greenish-gray sandy shale			XX	XX	XX				
Upper member†	439.3	GD1-35	Greenish-gray calcareous shale			XX	XX	XX				
Upper member†	451.4	GD1-36	Dark-gray calcareous silty shale			X	XX	XX				
Upper member†	454.5	GD1-37	Black calcareous shale			X	XXX	XX				
Upper member†	578.2	GD1-38	Greenish-gray calcareous sandstone			XX		XX				
Paradox Member†	949.1	+GD1-7	Dark-gray calcareous siltstone (5)#		X			o		XXX*		
Paradox Member†	976.3	+GD1-11	Orangish-red salt and carnallite (6)		o			o		XX		XXX
Paradox Member†	980.0	GD1-21	Red salt and carnallite (6)		XX			X		o		XXX
Paradox Member†	1027.4	GD1-8	Dark-gray silty dolomite (6)		XXX					XX		
Paradox Member†	1072.5	+GD1-9	Dark-gray dolomitic siltstone (8)		XX			X		XX		
Paradox Member†	1129.9	GD1-10	Black carbonaceous shale (9)		XXX			X		o		
Paradox Member†	1194.1	GD1-22	Orange sylvinite and anhydrite (13)		XX			X	X			XX
Paradox Member†	1204.6	GD1-19	Orange salt and anhydrite (13)		XX			o		XX*		XXX
Paradox Member†	1236.7	GD1-12	Black carbonaceous dolomitic shale (13)		XXX							
Paradox Member†	1347.5	GD1-20	Gray sylvinite and anhydrite (18)		XXX			XX		o		o
Paradox Member†	1351.8	GD1-23	Gray sylvinite and anhydrite (18)		XX			o		XX		X
Paradox Member†	1516.2	GD1-14	Dark-gray calcareous siltstone (19)		XXX			XX			X	
Paradox Member†	1521.7	+GD1-15	Calcareous siltstone and anhydrite (19)		XXX			XX				
Paradox Member†	1604.2	GD1-13	Calcareous sandy siltstone (21)		XXX			XX				
Lower member†	1678.8	GD1-2	Black calcareous carbonaceous shale		XXX			X				
Lower member†	1683.5	GD1-1	Black calcareous carbonaceous shale		XXX			XX				
Lower member†	1684.8	+GD1-3	Gray dolomitic siltstone		XXX			XX				
Lower member†	1686.2	GD1-4	Dark-gray dolomitic siltstone		XXX			XX			X	
Lower member†	1726.1	GD1-5	Dark-gray calcareous shale				XXX	XX				
Molas Formation	1741.3	+GD1-6	Greenish-gray calcareous shale				XXX	X				
Molas Formation	1752.0	+GD1-16	Red and green calcareous shale				XXX	X				
Molas Formation	1755.0	GD1-17	Red and green calcareous shale				XXX	X				
Molas Formation	1768.7	GD1-31	Purplish-gray calcareous shale				XX	XX				
Molas Formation	1780.5	+GD1-18	Red paleosol mudstone	XXX		X						

Clay minerals: kao-kaolinite; ill-illite; ils-mixed-layer illite with minor dioctahedral smectite; i-s-mixed-layer illite and dioctahedral smectite; chl-chlorite; c-s-mixed-layer chlorite and trioctahedral smectite; cor-corrensite and corrensite-like clay; sap-trioctahedral(?) smectite; tal-talc.

Qualitative abundances: XXX-major or dominant clay; XX-abundant clay; X-minor clay; o-minor and questionable clay constituent. All abundances relative to clay assemblage of that sample.

† The Hermosa Formation is subdivided into the lower member, Paradox Member, and upper member.

Parenthetical number designates salt depositional cycle in the Paradox Member (after Hite, 1960).

+ Chemical analysis of <1 μm fraction in table 2.

* Diffraction traces show superlattice reflections and basal reflections are rational within Bailey's (1982) limits (CV <0.75).

We have not attempted to rigorously quantify individual clay-mineral abundances within clay assemblages. Controversy over the reliability of such determinations and the additional uncertainties introduced by the presence of one or more abundant trioctahedral clays in many of these assemblages precluded making these measurements. On the other hand, we have estimated relative abundances of phases constituting the clay assemblage by visual inspection of peak intensities on diffraction traces in qualitative terms of "major constituent," "abundant constituent," "minor constituent," and "questionable constituent."

For selected samples, an aliquot of the aqueous suspension of the <1 μm fraction was dried, and the residue submitted to the U.S. Geological Survey's Denver analytical laboratories for major element determination using the X-ray fluorenscence technique of Taggart and others (1981) X-ray fluoresence technique. We also plan additional work on selected samples to include: measurement of the b-dimension of the clays using the 060 reflection; expansion measurements with glycerol; differential thermal analysis; and determination of cation exchange capacity.

CLAY-MINERAL ASSEMBLAGES

The results of diffraction studies for 37 samples from the core are compiled in table 1; eight of the samples have also been analyzed chemically for major element composition (table 2). Eight clay species were identified from these samples: kaolinite, illite, mixed-layer illite-dioctahedral smectite, chlorite, corrensite and corrensite-like clay, randomly interstratified chlorite-trioctahedral smectite, trioctahedral smectite (?saponite), and talc. We have arbitrarily subdivided the dioctahedral mixed-layer clays into two varieties based on the relative abundance of interstratified smectite in the clay (table 1).

Kaolinite is identified by its strict, nonexpandable 7 Å basal periodicity which is destroyed after heating at 550°C. Only when kaolinite is a minor constituent in a chlorite-rich assemblage does its presence become difficult to establish. The chemistry of a kaolinite-rich clay-mineral assemblage, such as in GD1-18 (table 2), is illustrated by its high-alumina content with negligible MgO, CaO, Na_2O, and K_2O. The high-ferric iron content results from abundant admixed hematite in the <1 μm fraction and substantial quartz accounts for the excess silica. Kaolinite is restricted to the Cutler Formation and red matrix muds in the paleosol facies of the lower Molas Formation (table 1).

Discrete illite is characterized by its symmetrical, usually sharp 10 Å 001 diffraction peak and rational higher order maxima; the basal reflections neither shift with glycol saturation nor are they affected by heat treatment. Sample GD1-15, an illite-rich clay assemblage with chlorite (table 1), contains the anticipated high-K_2O content (table 2). Stratigraphically, discrete illite is confined to the lower member and Paradox Member of the Hermosa Formation (table 1).

Randomly interstratified mixed-layer illite and dioctahedral smectite (the montmorillonite to beidellite series) was found throughout the stratigraphic sequence except in the Paradox Member. Two types can be

Table 2.--*Chemical analyses (weight percent) of insoluble <1 μm effective spherical diameter fractions of the Molas, lower member, and Paradox Member of the Hermosa Formation from Gibson Dome No. 1 drill core, San Juan County, Utah*

[Analyst: U.S. Geological Survey Laboratory, Denver.]

	Molas Formation			Lower member Hermosa Fm.	Paradox Member, Hermosa Formation			
Depth (m)	1780.5	1752.0	1741.3	1684.81	1521.7	1072.5	976.3	949.1
Sample no.	GD1-18	GD1-16	GD1-6	GD1-3	GD1-15	GD1-9	GD1-11	GD1-7
SiO_2	48.3	47.8	50.7	45.5	47.2	41.6	42.9	39.0
TiO_2	1.11	0.91	0.72	0.89	0.48	0.37	0.15	0.37
Al_2O_3	26.9	22.8	22.1	15.4	20.1	15.9	9.31	12.5
Fe_2O_3 (1)	11.0	7.99	6.35	7.16	3.57	5.16	2.00	4.40
MnO	<0.02	<0.02	<0.02	<0.02	<0.02	<0.02	<0.02	<0.02
MgO	0.70	4.63	3.15	14.4	11.6	17.0	30.7	26.5
CaO	<0.02	<0.02	<0.02	0.60	0.60	0.80	<0.02	0.70
Na_2O	0.91	1.53	1.93	0.31	0.28	0.68	0.79	0.97
K_2O	0.76	3.50	3.83	3.76	5.37	3.58	0.11	0.87
P205	0.06	<0.05	<0.05	0.21	0.20	0.57	<0.05	0.38
LOI (2)	10.6	11.0	11.1	11.3	10.1	13.6	13.2	13.6
Total	100.4	100.2	99.9	99.5	99.5	99.3	99.2	99.3

(1) Total iron as Fe_2O_3.
(2) Loss on ignition at 900°C.

distinguished; one contains less than 10 percent interstratified smectite, and the other contains as much as about 40 percent smectite.

The former is characterized by a slightly expanded air-dried 001 reflection at 10.3-10.6 Å; the peak is somewhat asymmetrical with a distinct low-angle tail. With glycol saturation, a sharp peak develops at the characteristic 9.9-10.0 Å mica spacing, but the low-angle tail becomes even more pronounced. Reynolds (1980) interpreted these features as indicative of an illite containing only minor (less than 10 percent) interstratified smectite layers. This variety is dominant in the Cutler Formation sediments and is also present, but less abundantly, in the upper member of the Hermosa Formation (table 1).

The second mixed-layer variety is characterized by an even more greatly expanded air-dried 001 reflection (10.8-11.4 Å). With glycol saturation the diagnostic maxima occur at 9.2-9.6 Å and 5.22-5.28 Å which correspond to a clay with 30-40 percent smectite layers (Reynolds, 1980). Clays of this composition are abundant in the Molas Formation and lowermost lower member of the Hermosa Formation. They also occur coexisting with the more illite-rich variety in the upper member. Sample GD1-6 has 3.83 weight percent K_2O (table 2), and diffraction results suggest an assemblage of nearly monomineralic mixed-layer illite-smectite with only minor chlorite (table 1). Since a discrete illite is expected to contain 8 percent or more K_2O, the mixed-layer character of this clay becomes apparent.

Chlorite is characterized by a well-developed 14 Å periodicity which does not expand with glycol saturation. After heat treatments no major shifts are observed, although at 550°C the basal 001 spacing does collapse slightly (13.5-13.8Å) and is strongly enhanced whereas intensities of the higher order reflections are substantially diminished. Chlorite is common throughout the section except for its reduced abundance in the upper two-thirds of the Paradox Member and the upper beds of the Cutler Formation, and its absence in Molas paleosols (table 1). The occurrence of moderate-to-appreciable MgO in GD1-16, GD1-15, and GD1-3 (table 2) reflects the presence of variable proportions of chlorite.

We are defining corrensite as a regularly interstratified 1:1 chlorite and trioctahedral expandable clay to avoid any confusion with the current controversy as to whether or not the expandable layer must be or can be smectite, vermiculite, or "expandable" chlorite, and as to whether or not the expandable layer must be trioctahedral. An ideal corrensite yields a rational series of higher order basal reflections with a 001 spacing of ~29Å for air-dried material, ~30-31Å if glycol saturated, and ~24Å after heating to 550°C. Deviation from the 1:1 composition and from regular interstratification yields nonrational higher-order reflections, as well as variations in the superlattice spacing with the different sample treatments.

In our samples, we tentatively identify the expandable layer as a smectite, presumably saponite, on the basis of the character of the expansion with ethylene glycol and collapse after heating at 550°C; unequivocal discrimination between saponite and vermiculite requires glycerol saturation.

Table 3.--*Spacings (Angstroms) of 001 diffraction maxima from glycol-saturated "corrensites" in the Hermosa Formation from Gibson Dome No. 1 drill core, San Juan County, Utah; the c_o-dimension is the mean of calculated values from d_{001} measurements with standard deviation, s, and coefficient of variation, CV*

	Upper member		Paradox Member				
Sample no.	GD1-33	GD1-7	GD1-11	GD1-8	GD1-9	GD1-19	GD1-23
Depth (m)	384.4	949.1	976.3	1027.4	1072.5	1204.6	1351.8
hkl							
001	31.6	30.5	31.6	30.5	31.6	31.6	30.5
002	15.0	15.5	15.2	15.1	14.5	15.5	15.0
003	#	#	#	#	#	10.40	#
004	7.44	7.66	7.70	7.38	7.70	7.81	7.76
005		6.19			6.33	6.24	
006	5.16	5.13	5.14	4.98	5.13	5.16	5.22
007	4.42	4.42	4.46		4.40	4.45	
008	3.83	3.87				3.87	
009	3.48	3.45	3.46	3.51	3.45	3.46	3.47
00.10		3.11	3.12			3.14	
00.11	2.831	2.814	2.823	2.840	2.823	2.823	2.823
00.12							
00.13			2.350	2.368			
00.14							
00.15		2.067	2.062	2.049		2.067	
c_o	30.78	30.89	30.98	30.55	30.83	31.66	30.84
s	0.59	0.19	0.33	0.68	0.82	0.18	0.52
CV	1.9	0.62	1.1	2.2	2.7	0.57	1.7

Unresolved due to interference with d_{001} of illite.

We have characterized the trioctahedral clay constituent as "corrensite" in table 1 if a recognizable 001 superlattice reflection is observed in the 3° 2θ region. Thus, our "corrensite" ranges from true corrensite with nearly ideally regularly interstratified chlorite-expandable clay layers and a 1:1 composition as defined by Bailey (1982) to a mixed-layer chlorite-expandable clay with imperfect interstratification, but which still produces superlattice reflections. Those "corrensites" in table 1, which, in addition to yielding diagnostic superlattice reflections, also generated sufficient rationality of higher orders (a coefficient of variation <0.75) to justify identification as a true corrensite are flagged with an asterisk. The basal spacings ($d_{00\ell}$) of "corrensites" in seven glycol-saturated samples which contain sufficient "corrensite" to yield measurable higher order (>002) maxima are given in table 3, and generate coefficients of variation from 0.57 to 2.7. "Corrensite" is restricted to the Paradox Member and one occurrence in the upper member (table 1).

Two analyzed "corrensite"-rich samples (GD1-7, 11; table 2) exhibit the expected high MgO and correspondingly low Al_2O_3. Although the GD1-11 assemblage consists chiefly of talc with coexisting abundant corrensite and minor illite (table 1), diffraction traces of the <1 μm fraction show only negligible quantities of talc and illite with the corrensite; talc was effectively isolated in the >1 μm fraction. Recognizing that possible errors may be introduced by the two minor phases with the corrensite, we have recast the chemical analysis of the <1 μm fraction of GD1-11 (table 2) to the corrensite structural formula (table 4) after arbitrarily assigning all iron as FeO. The eight tetrahedral sites occur as a pair of sites in each of four tetrahedral sheets--two sheets in the 2:1 smectite layer and two sheets in the chlorite 2:1 layer. A total of nine octahedral sites occur: three in the octahedral sheet of the smectite layer; three in the octahedral sheet of the chlorite 2:1 layer; and three in the separate brucite-like sheet of the chlorite structure. A small, but variable number of cation sites also occur in the smectite interlayer position.

The stoichiometry (table 4) closely approaches that of an ideal corrensite. The chlorite layer undoubtedly contains most, if not all of the tetrahedral aluminum; this would yield slightly more than three silicons per four tetrahedral sites in the chlorite--a clinochlore composition. Essentially all of the octahedral aluminum is assigned to the chlorite and would be distributed between the octahedral sheet in the 2:1 layer and the brucite-like sheet. The trioctahedral smectite would be expected to contain little, possibly no tetrahedral aluminum and essentially no octahedral aluminum. As 8.81 out of 9.00 octahedral sites in the combined chlorite-smectite pair are occupied (table 4), the likelihood exists of incomplete occupancy in the smectite octahedral sheet. This would give the smectite layer a stevensite-like character and would contribute to the charge deficiency in the 2:1 layer required to balance the positive charge of the smectite's interlayer cations.

Two other expandable trioctahedral clays also occur, but only infrequently. A chlorite-rich clay with randomly interstratified trioctahedral (?saponite) layers is observed as a minor constituent in one sample (GD1-22). Diffraction maxima at 15.4, 7.55, and 3.52 Å after glycol saturation, and the total absence of superlattice reflections regardless of sample treatment suggest random interstratification of 60-70 percent chlorite layers with 40-30 percent smectite layers (Reynolds, 1980). Its host lithology is a sylvinite from the

Table 4.--*Structural formula of corrensite from the Paradox Member of the Hermosa Formation calculated from chemical analysis of GD1-11 <1 m fraction (table 2) for 25 oxygens (14 in chlorite, 11 in smectite) with iron as FeO*

Tetrahedral:[1]	Si^{4+}	7.12
	Al^{3+}	.88
Total		8.00
Octahedral:[2]	Al^{3+}	.95
	Ti^{4+}	.02
	Fe^{2+}	.25
	Mg^{2+}	7.59
Total		8.81
Interlayer:[3]	Na^{+}	.26
	K^{+}	.02
Total		0.28

Tetrahedral charge deficiency:	-0.88
Octahedral charge excess:	+0.61
Interlayer charge excess:	+0.28

1 Two sites in each of four sheets: two sheets in smectite 2:1 layer; two sheets in chlorite 2:1 layer.

2 Three sites in each of three sheets: one sheet in smectite 2:1 layer; one sheet in chlorite 2:1 layer; one sheet in chlorite brucite-like sheet.

3 Smectite interlayer sites.

Paradox Member where it is associated with abundant illite and talc, and minor discrete chlorite (table 1). The second species is a discrete smectite that fully expands to 16.5-17 Å after glycol saturation and collapses to 9.4-9.7 Å after heating. It occurs as a minor constituent in two siltstones, GD1-4 from the upper member and GD1-14 from the Paradox Member, and coexists with abundant illite and appreciable discrete chlorite (table 1).

Talc is characterized by a strictly rational series of basal reflections at 9.4 Å that neither expand with glycol saturation nor are affected by heat treatment. Talc is confined to, and commonly very abundant in rock salt and potash-bearing salt strata in the Paradox Member, but is absent from associated anhydrite, carbonate, and clastic lithologies (table 1). It is typically coarser grained than its associated clays such that its relative abundance is greatly reduced in the <1 μm fraction.

DISCUSSION

The succession of clay-mineral assemblages in the Gibson Dome No. 1 core well illustrates the important role that depositional environment plays in controlling clay mineral speciation. Depositional conditions range from residual soil (lowermost Molas Formation), eolian, and fluvial (upper Cutler Formation) continental environments through nearshore mixed marine and continental environments (lower Cutler Formation), normal marine environments (upper two-thirds of the Molas Formation and the upper part of the upper member of the Hermosa Formation), and transitional environments between marine and hypersaline (lower and lowermost upper members of the Hermosa Formation) to marine hypersaline environments (Paradox Member of the Hermosa Formation).

Throughout this discussion the term "depositional environment" is expanded to include the early diatgenetic environment in which the physical and chemical parameters, that is, temperature, pressure, and pore fluid composition, are derived from and remained similar to those existing at the time of deposition. Because clay-mineral reactions are characteristically slow at surficial temperatures and because the time interval of deposition is short in contrast to the time interval during which early diagenesis would occur, it is likely most clay-mineral response to the "depositional environment" would occur during early diagenesis rather than curing the strict interval of deposition.

The continental strata characteristically contain kaolinite-bearing assemblages. Kaolinite is dominant in the paleosol of the Molas Formation (GD1-18, table 1), and the clay-size fraction has a highly aluminous composition (table 2) with only negligible quantities of the alkalies and alkaline earths; the high-iron content reflects the abundance of hematite associated with the kaolinite. This analysis is very similar to some residual clay analyses compiled in Pettijohn (1975) and reflects intense weathering and leaching of the limestone residuum.

Kaolinite also occurs as a major constituent in the upper or continental interval of the Cutler Formation; the clay assemblages contain abundant mixed-layer illite-dioctahedral smectite, and occasional minor chlorite along with the kaolinite (GD1-24, 28; table 1). Kaolinite also occurs in the mixed marine-continental strata of the lower Cutler Formation, although its relative abundance is markedly lower (GD1-25, 26, 29, 30; table 1). In these samples,

increasing chlorite abundance parallels decreasing kaolinite abundance downward with increased marine influence in the depositional environment; the major constituent throughout remains mixed-layer illite-smectite.

Possibly changing provenance, such as source rock lithology and its in-place weathering, and changing mechanical processes in the depositional environment, such as particle-size segregation in response to currents and distance from the site of detrital influx, contribute to the observed clay-mineral variation between the upper and lower Cutler Formation assemblages (table 1). We suggest two other factors. Both focus on the chemistry of the depositional environment: the freshwater and commonly slightly acidic character of the upper Cutler Formation continental depositional environments as opposed to the marginally to moderately saline (to seawater composition) and somewhat alkaline character of nearshore mixed marine-continental depositional environments for the lower Cutler Formation. First, deposition in the upper Cutler Formation environments would have promoted continued leaching and degradation of accumulating clay detritus toward a more kaolinite-rich assemblage at the expense of the remaining more aggraded species. Deposition in the lower Cutler Formation environments, on the other hand, would have tended to arrest the clay-degradation process; kaolinite would have ceased forming, and the remaining more aggraded detrital clays, such as soil chlorites or vermiculites, and mica-clays, as well as inherited clays from any clay-bearing source rocks, would have tended to have been preserved. Second, any kaolinite or other highly degraded species would have been out of equilibrium upon entering the more saline environments of lower Cutler Formation deposition and early diagenesis; the degraded clays would dissolve or would have tended to recrystallize to more aggraded species such as a mixed-layer illite-smectite.

In marine strata, mixed-layer illite-smectite is the dominant species coexisting with variable quantities of chlorite. Kaolinite is absent. These assemblages characterize all normal marine intervals of the studied section (table 1). Samples from the Ouray and Leadville Limestones are currrently being analyzed; results are not available. Two chemical analyses of the <1 μm fraction from the marine Molas Formation (GD1-6, 16; table 2) show moderately high Al_2O_3, with moderate amounts of MgO, Na_2O, and K_2O; these compositions are similar to marine shale and mud compositions as compiled, for example, in Pettijohn (1975), except for our decreased SiO_2 and CaO values reflecting removal of quartz and carbonate minerals during clay-fraction separation.

Of the intervals reflecting the transition from marine to hypersaline (lower member of the Hermosa Formation) and from hypersaline to marine (lower upper member), only the lower member results are available. The most notable mineralogic change in the clay assemblage is the appearance of a discrete illite rather than the mixed-layer clay; in some samples an increased chlorite abundance also occurs (table 1). A chemical analysis of one clay-size separate from the lower member (table 2) shows substantially lower alumina and higher magnesia than in the marine Molas Formation. This is due to increased abundance of chlorite in the clay assemblage, and reflects the increasingly magnesium-rich brine in the depositional environment and its interaction with detrital clays.

The hypersaline strata of the Paradox Member of the Hermosa Formation continue the trend to more magnesian-rich clay assemblages. In addition to increasing chlorite abundance in some samples, talc, corrensite, and corrensite-

like clay commonly occur and become dominant in several samples (table 1). In a few samples, randomly interstratified chlorite-trioctahedral smectite or discrete smectite are observed. Only discrete illite remains as an aluminum-rich phase; kaolinite and interstratified clays containing dioctahedral smectite are absent. Similar assemblages have been described from several marine evaporite sections (Füchtbauer and Goldschmidt, 1959; Braitsch, 1971; Millot, 1970; Bodine, 1978; Bodine and Standaert, 1977), and appear to be characteristic of clay assemblages that evolved from detritus deposited in the marine hypersaline environment.

An additional mineralogic feature of the Paradox Member clay assemblages is the restriction of talc to the saline lithologies (rock salt, sylvinite, etc.), and its absence in intercalated anhydrites, carbonates, and clastics (table 1). This conforms to similar relations in the German Zechstein (Braitsch, 1971) and the New Mexico Salado Formation (Bodine, 1979), and strongly suggests neoformation of talc in Mg-rich marine hypersaline brine environments in response to equilibria in the MgO-SiO_2-H_2O system (Bricker and others, 1973).

The chemistry of the Paradox Member clay assemblages closely parallels clay mineral distribution. An assemblage with dominant illite and low-to-moderate amounts of the trioctahedral clays has moderate Al_2O_3, very high K_2O, and, for hypersaline clays, only moderate MgO content (GD1-15; tables 1 and 2). On the other hand, the two assemblages, GD1-7 and GD1-11, that are overwhelmingly dominated by triocthedral clays with substantially lower illite abundance (table 1), are severely depleted in Al_2O_3 and K_2O but are greatly enriched in MgO (table 2).

One anomolous sample is GD1-33 occurring toward the top of the upper member of the Hermosa Formation. Its clay assemblage (table 1) is characteristic of having formed in the marine hypersaline environment. Corrensite is the dominant clay, and it coexists with a relatively minor amount of a mixed-layer illite-dioctahedral smectite; the assemblage differs markedly from the typical marine clay assemblages observed in the other five samples from the upper member of the Hermosa Formation. One tentative explanation is that during the final stages of deposition in the Pennsylvanian seaway, sabkha or even local ephemeral evaporite brine environments formed on isolated nearshore areas, and the sample represents response to such an environment.

Late diagenetic effects accompanying deep burial ("burial metamorphism" after Hower and others, 1976), sediment dewatering (compaction), and, particularly in the more permeable strata, the migration of transient pore fluids through deep-basin aquifers, also played an important role. It appears likely that isochemical or nearly isochemical recrystallization of clays, such as the transformation to corrensite from randomly interstratified mixed-layer clays, occurred only after substantial burial and a modest temperature increase. The anomolous occurrence of a trioctahedral clay-rich assemblage (sample GD1-33, table 1) in the overlying upper member of the Hermosa Formation, which, as explained in the preceding paragraph, could be tentatively attributed to an ephemeral depositional phenomenon, can alternatively be a late diagenetic event. The assemblage may reflect alteration of a preexisting dioctahedral, normal marine assemblage through interaction with migrating hypersaline brines that were expelled from compacting underlying saline beds of the Paradox Member into this more permeable horizon of the overlying marine unit.

NUCLEAR WASTE STORAGE AND HOST-ROCK CLAYS

Underground emplacement of nuclear waste will have two major effects that might result in altering the host-rock clay minerals: (1) clay reactions caused by heat of radioactive decay that will produce a thermal envelope around the waste source; and (2) clay reactions caused by clay mineral interaction with any effluent escaping from the waste containers.

Thermal effects on clays at relatively low temperatures (<200°C) are restricted chiefly to the release of unbound molecular water in clays (Grim, 1968). Such reactions do not involve structurally bound water, but are restricted to expulsion of interlayer and other sorbed molecular water. All clays at ambient temperature will have some water of this type, and the amount only becomes substantial (5-15 weight percent of the clay) in those clays that contain one or more sheets of molecular interlayer water. Of the Paradox Member clays, only smectite (or vermiculite), occurring chiefly as layers in corrensite and other instrastratified chlorite-trioctahedral smectite clays, contains interlayer water molecules. A second consideration at or near these temperatures is the transformation of the smectite interlayers to discrete chlorite. If the reaction does occur at a reasonable reaction rate, it will either consume free water or convert the smectite's molecular interlayer to form the additional structural water required to construct the chlorite layer's brucite-like sheet from the smectite.

In the temperature range of 200°-500°C, a variety of clay-to-clay transformations may occur; the character and extent of such reactions depend upon temperature, pressure, composition of the reactant assemblage, and chemistry of the pore fluids (Velde, 1977). Of the Gibson Dome No. 1 clays, the illite-chlorite assemblage with or without talc would most likely be the assemblage with the greatest thermal stability. Expulsion of structural water from the clays can begin at temperatures no lower than 400°-500°C and continue to about 700°-800°C; the specific temperature interval is a function of the particular clay mineral involved (Grim, 1968). In such reactions, the clay structure is destroyed, structural water is expelled, and an assemblage of anhydrous silicate phase remains.

Any thermal anomaly surrounding the waste may also result in reactions in the host salts themselves, such as release of fluid-inclusion water from salts, and dehydration, even recrystallization, of selected minor evaporite minerals in the salt assemblage. If such thermally induced reactions produce severe pH or dissolved salt concentration changes in the ambient pore fluid, the fluid equilibria with clays may be shifted, and compensating clay dissolution, hydrolysis, and ion exchange reactions may occur.

The potential effects of interaction between the clay minerals and any waste effluent escaping from the containers must also be considered. Some possibilities include: the anion character of the effluent, particularly if it contains certain organic-acid complexes such as EDTA, may greatly increase clay-mineral solubility (Malcolm and others, 1975); extreme pH's of the effluent, whether acidic or basic, may cause one or more of a wide array of clay dissolution or hydrolysis reactions, particularly at elevated temperatures (Velde, 1977); and radioactive cations in the effluent, such as cesium or strontium, may result in their sorption into interlayer cation sites of smectite

(or vermiculite) through ion exchange (Grim, 1968).

To a large extent, these potential clay reactions, whether due to thermal perturbation or excaping effluent, or both, are likely to result in little more than negligible overall alteration of the repository host at this site; the clay content in salt 6 is small (R. J. Hite, oral commun.). Were any of these reactions, however, to extend into the neighboring clay-rich black shale interbeds, the alteration of the shale might be substantial. The chemical and mineralogic properties of the shale, as well as its physical properties (such as permeability) might be changed dramatically.

REFERENCES

Bailey, S. W., 1982, Nomenclature for regular interstratifications: American Mineralogist, v. 67, p. 394-398.

Bodine, M. W., Jr., 1978, Clay-mineral assemblages from drill core of Ochoan evaporites, Eddy County, New Mexico, in Austin, G. S., ed., Geology and Mineral Deposits of Ochoan Rocks in Delaware Basin and Adjacent Areas: New Mexico Bureau of Mines and Mineral Resources, Circular 159, p. 21-31.

Bodine, M. W., Jr., and Fernalld, T. H., 1973, EDTA dissolution of gypsum, anhydrite, and Ca-Mg carbonates: Journal of Sedimentary Petrology, v. 43, p. 1152-1156.

Bodine, M. W., Jr., and Standaert, R. R., 1977, Chlorite and illite compositions from Upper Silurian rock salts, Retsof, New York: Clays and Clay Minerals, v. 25, p. 57-71.

Braitsch, Otto, 1971, Salt Deposits, their Origin and Composition: New York, Springer-Verlag, 297 p.

Bricker, O. P., Nesbitt, H. W., and Gunter, W. D., 1973, The stability of talc: American Mineralogist, v. 58, p. 64-72.

Brindley, G. W., and Brown, George, eds., 1980, Crystal Structure of Clay Minerals and their X-ray Identification: London, Mineralogical Society Monograph 5, 495 p.

Carroll, Dorothy, 1970, Clay Minerals: a Guide to their Identification: Geological Society of America Special Paper 126, 80 p.

Füchtbauer, H., and Goldschmidt, H., 1959, Die Tonminerale der Zechsteinformation: Beitrage zur Mineralogie und Petrogrophie, v. 6, p. 320-345.

Grim, R. E., 1968, Clay Mineralogy (2nd ed.): New York, McGraw-Hill Book Co., 596 p.

Hite, R. J., 1960, Stratigraphy of the saline facies of the Paradox Member of the Hermosa Formation of southeastern Utah and southwestern Colorado, in Geology of the Paradox Basin Fold and Fault Belt, 3rd Field Conference Durango, Colorado: Four Corners Geological Society, p. 86-89.

Hite, R. J., 1983, Preliminary mineralogical and geochemical data from the D.O.E. Gibson Dome Corehole No. 1, San Juan County, Utah: U.S. Geological Survey Open-File Report 83-780, 10p.

Hite, R. J. and Buckner, D. H., 1981, Stratigraphic correlations, facies concepts, and cyclicity in Pennsylvanian rocks of the Paradox Basin, in Wiegand, D. L., ed., Geology of the Paradox Basin: Rocky Mountain Association of Geologists Field Conference, p. 147-160.

Hower, John, Eslinger, E. V., Hower, M. E., and Perry, E. A., 1976, Mechanism of burial metamorphism of argillaceous sediment: Mineralogical and chemical evidence: Geological Society of America Bulletin, v. 87, p. 725-737.

Malcolm, R. L., Leenheer, J. A., and Weed, S. B., 1975, Dissolution of aquifer clay mineral during deep well disposal of industrial organic waste, in International Clay Conference Proceedings, Mexico City, Mexico: p. 477-493.

Millot, Georges, 1970, Geology of Clays: New York, Springer-Verlag, 429 p.

Pettijohn, F. J., 1975, Sedimentary Rocks (3rd ed.): New York, Harper & Row, 628 p.

Pollastro, R. M., 1982, A recommended procedure for the preparation of oriented clay mineral specimens for X-ray diffraction analysis: modifications to Drever's filter-membrane peel technique: U.S. Geological Survey Open-File Report 82-71, 10 p.

Reynolds, R. C., 1980, Interstratified clay minerals, in Brindley, G. W. and Brown, George, eds., Crystal Structures of Clay Minerals and their X-ray Identification: London, Mineralogical Society Monograph 5, p. 249-304.

Taggart, J. E., Jr., Lichte, F. E., and Wahlberg, J. S., 1981, Methods of analysis of samples using X-ray fluoresence and induction-coupled plasma spectroscopy, in Lipman, P. W. and Mullineaux, D. R., eds., The 1980 Eruptions of Mount St. Helens, Washington: U.S. Geological Survey Professional Paper 1250, p. 683-687.

Velde, Bruce, 1977, Clays and clay minerals in natural and synthetic systems: New York, Elsevier Scientific Publishing, 218 p.

Wengerd, S. A., 1958, Pennsylvanian stratigraphy, southwest shelf, Paradox basin, in Intermountain Association Petroleum Geologists Guidebook 9th Annual Field Conference, Guidebook to the Geology of the Paradox Basin: p. 109-134.

Woodward-Clyde Consultants, 1982, Geologic characterization report for the Paradox Basin study region, Utah study areas, Vol. II, Gibson Dome: Office of Nuclear Waste Isolation, ONWI-290.